# Aluminum Fluoride Activation of Bovine Transducin Induces Two Distinct Conformational Changes in the $\alpha$ Subunit†

Rohit Mittal, Richard A. Cerione, and Jon W. Erickson*

*Department of Pharmacology, Schurman Hall, Cornell University, Ithaca, New York 14853-6401*

*Received April 11, 1994; Revised Manuscript Received June 15, 1994®*

ABSTRACT: We have used resonance energy transfer to read out the interactions of the $\alpha$ subunit of transducin ($\alpha_T$) with the transducin $\beta\gamma$ subunit complex ($\beta\gamma_T$) and to compare the rate of aluminum fluoride-induced $\alpha_T$ activation, as reflected by the enhancement of the $\alpha_T$ tryptophan fluorescence, with the rate for the dissociation of holotransducin into its component subunits. Specifically, a $\beta\gamma_T$ complex that was labeled with 5-(iodoacetamido)fluorescein (IAF-$\beta\gamma_T$) served as a donor for resonance energy transfer and an $\alpha_T$-GDP species labeled with eosin 5-isothiocyanate (EITC-$\alpha_T$GDP) served as the acceptor. The quenching of IAF-$\beta\gamma_T$ fluorescence emission by the addition of the EITC-$\alpha_T$GDP species, due to resonance energy transfer between the IAF and EITC moieities, ranged from 10% to 15%. The association of the transducin subunits was rapid (i.e., within the time period of mixing) and dose-dependent, yielding an apparent $K_d$ of ~150 nM for the $\alpha_T$GDP/$\beta\gamma_T$ interaction. Unexpectedly, we find that the dissociation of IAF-$\beta\gamma_T$ from an aluminum fluoride-activated $\alpha_T$GDP/IAF-$\beta\gamma_T$ complex occurs prior to the onset of the intrinsic fluorescence changes in $\alpha_T$ that accompany activation of this subunit. Thus, there are at least two structural changes in $\alpha_T$ that result from the occupation of the $\gamma$-phosphate position in the nucleotide binding cleft of $\alpha_T$ by aluminum fluoride. These structural changes result in two kinetically distinguishable states that correspond to $\beta\gamma_T$ dissociation and to the priming of $\alpha_T$ for coupling to the effector enzyme, respectively.

The vertebrate vision system represents an excellent model for receptor/G protein-coupled signal transduction (Stryer, 1991; Khorana, 1992). This signaling cascade is initiated by the absorption of light by the photoreceptor, rhodopsin, in the outer segments of mammalian rod cells. The light-activation event promotes the interaction of rhodopsin with the heterotrimeric G protein holotransducin and results in the exchange of GTP for tightly bound GDP on the $\alpha$ subunit ($\alpha_T$)[1] of the G protein. The GDP–GTP exchange results in a conformational change in the $\alpha_T$ subunit, typically referred to as the activation event, that enables the $\alpha_T$ subunit to bind to its target effector enzyme, the retinal cyclic GMP phosphodiesterase (PDE), and stimulate the hydrolysis of cyclic GMP to 5′-GMP. It is the reduction in the levels of cyclic GMP that causes the closure of $Na^+$ channels in the retinal rod membrane; this hyperpolarization represents the signal that is conveyed to the optic nerve. The active $\alpha_T$GTP species continues to stimulate PDE through its interaction with the inhibitory PDE $\gamma$ subunit ($\gamma$ PDE) until a GTPase activity, which is intrinsic to the $\alpha_T$ subunit but is thought to be additionally stimulated by $\gamma$ PDE (Arshavsky & Bownds, 1992), returns the $\alpha_T$ subunit to its GDP-bound state, thereby terminating the stimulation of the effector enzyme.

One approach to studying this complex system of protein–protein interactions has relied on the development of sensitive, real-time measurements of the interactions between highly purified retinal components. A long-term goal of this laboratory has been to develop fluorescence assays for monitoring individual steps that comprise this receptor/G protein-mediated signaling cascade. The intrinsic tryptophan fluorescence of the $\alpha_T$ subunit has served as a sensitive monitor for conformational changes in the $\alpha_T$ subunit that accompany rhodopsin-stimulated GTP binding and aluminum fluoride-induced activation (Phillips & Cerione, 1988; Guy et al., 1990). It has recently been shown that this change in intrinsic fluorescence is due solely to an increase in $\alpha_T$ tryptophan 207 fluorescence (Faurobert et al., 1993). Environmentally sensitive fluorescent reagents such as 2-(4′-maleimidoanilino)-naphthalene-6-sulfonic acid (MIANS) can be attached to the cysteine residues of the $\beta\gamma_T$ subunit complex and used as reporter groups to monitor rhodopsin/$\beta\gamma_T$ (Phillips & Cerione, 1992) and $\alpha_T/\beta\gamma_T$ interactions (Phillips & Cerione, 1991). In addition, we have labeled the reactive lysine residue on the $\alpha_T$ subunit and the cysteine residues on the PDE with donor–acceptor pairs in order to use resonance energy transfer approaches to monitor $\alpha_T$/PDE interactions (Erickson & Cerione, 1991).

As we describe below, one mechanistic question of particular importance that is amenable to spectroscopic approaches concerns the kinetics of the G protein subunit dissociation process. Current models of G protein/effector interactions frequently depict the free $\alpha_T$GTP species, i.e., that which has dissociated from the receptor and the G protein $\beta\gamma_T$ subunit complex, as the species that mediates the regulation of the effector protein. If generation of a free, activated species is a necessary step in the transduction sequence, then the dissociation of the activated $\alpha_T$ subunit from the $\beta\gamma_T$ complex should be a rapid consequence of the activating conformational change that is induced within the $\alpha_T$ subunit by GTP binding or by the coupling of aluminum fluoride (Higashijima et al., 1987) to the bound GDP molecule (i.e., to form an $\alpha_T$GDP/aluminum fluoride species). In this work we present data suggesting that aluminum fluoride induces two kinetically distinguishable conformational changes in holotransducin. The

† This research was support by National Institutes of Health Grant EY06429.

* To whom correspondence should be addressed.

® Abstract published in *Advance ACS Abstracts,* August 1, 1994.

[1] Abbreviations: $\alpha_T$, $\alpha$ subunit of transducin; $\beta\gamma_T$, transducin $\beta\gamma$ subunit complex; EITC-$\alpha_T$GDP, purified eosin 5-isothiocyanate conjugate of $\alpha$-transducin; IAF-$\beta\gamma_T$, 5-(iodoacetamido)fluorescein-labeled $\beta\gamma$ subunit complex of transducin; PDE, phosphodiesterase; $\gamma_{PDE}$, $\gamma$ subunit of phosphodiesterase; MIANS, 2-(4′-maleimidoanilino)naphthalene-6-sulfonic acid; ROS, rod outer segment; HEPES, *N*-(2-hydroxyethyl)-piperazine-*N*′-2-ethanesulfonic acid; DTT, dithiothreitol.

0006-2960/94/0433-10178$04.50/0 

first of these results in the rapid dissociation of the $\alpha_T$ subunit from the $\beta\gamma_T$ complex, and the second reflects changes in the environment of the tryptophan 207 residue that results in its enhanced fluorescence and may coincide with the priming of the $\alpha_T$ subunit for coupling to the effector enzyme.

## MATERIALS AND METHODS

*Purification of Retinal Proteins.* Frozen, dark-adapted bovine retina were obtained from Hormel (Austin, MN) and rod outer segment (ROS) membranes were isolated as described by Gierschik et al. (1984). Holotransducin was purified from ROS membranes essentially as outlined in Phillips et al. (1989). Specifically, the ROS membranes were exposed to room light, washed (5×) with 10 mM HEPES, pH 7.5, 6 mM $MgCl_2$, 1 mM DTT, plus 0.15 M NaCl (isotonic buffer) and then washed (5×) with the same buffer minus the NaCl (hypotonic buffer). The holotransducin was eluted from the membranes by suspending the pellets in hypotonic buffer supplemented with 0.1 mM GTP. Blue Sepharose chromatography (Pines et al., 1985) was then performed on the supernatants in order to resolve the $\beta\gamma_T$ subunit complex from the $\alpha_T$ subunit. We have shown that the majority of the $\alpha_T$ subunits that are purified in this manner contain tightly bound GDP (Kroll et al., 1989); thus, the $\alpha_T$ subunit is referred to as $\alpha_T$GDP throughout the text. The purified $\alpha_T$GDP and the $\beta\gamma_T$ complex were stored at concentrations of ~0.5–1 mg/mL at −20 °C in 10 mM HEPES, pH 7.5, 120 mM NaCl, 6 mM $MgCl_2$, 1 mM DTT, and 40% glycerol.

*Protein Modifications.* The modification of the reactive lysine residue on the $\alpha_T$GDP subunit was carried out as described previously (Erickson & Cerione, 1991). Typically, 500 μL of an ~0.5 mg/mL solution of the purified $\alpha_T$GDP was mixed with EITC (10 μL from a 25 mM stock solution in dimethyl sulfoxide) for ~2 h at room temperature. After this incubation, the reaction mixture was then applied to a hydroxyapatite column (600 μL) that had been preequilibrated with 10 mM $K_2HPO_4$ (pH 7.5). The column was washed several times to be certain that all of the unreacted EITC was removed and then the EITC-labeled $\alpha_T$GDP was eluted from the column with 100 mM phosphate. The EITC-$\alpha_T$GDP was then dialyzed overnight (4 °C) versus 20 mM HEPES, pH 7.4, 5 mM $MgCl_2$, 1 mM DTT, and 150 mM NaCl plus 40% glycerol. The stoichiometry of EITC per $\alpha_T$GDP was ~1 based on protein determinations using the $Cu^+$/bicinchoninic acid method (with bovine serum albumin as a standard) and the absorbance of the EITC moiety ($\epsilon_{max,523nm}$ = 86 000 $M^{-1}$ $cm^{-1}$).

The modification of the $\beta\gamma_T$ subunit complex with IAF was performed as follows. The purified $\beta\gamma_T$ complex was first dialyzed versus 20 mM HEPES, pH 7.5, 5 mM $MgCl_2$, 0.15 M NaCl, and 20% glycerol to remove the DTT from the $\beta\gamma_T$ storage buffer. The dialyzed $\beta\gamma_T$ (~0.5 mL of a 0.5 mg/mL protein stock solution) was mixed with IAF (10 μL of a 25 mM stock solution in dimethylfuran). The reaction was carried out for ~3 h at room temperature. The reaction mixture was then applied to a hydroxyapatite column preequilibrated with 10 mM potassium phosphate (pH = 7.5), which was washed to remove the unreacted probe, and then the IAF-labeled $\beta\gamma_T$ was eluted with 100 mM potassium phosphate, pH 7.4. The stoichiometry of IAF labels per $\beta\gamma_T$ was consistently found to be ~3:1 based on the $Cu^+$/bicinchoninic acid protein determination and an extinction coefficient at 492 nm for IAF of 74 000 $M^{-1}$ $cm^{-1}$.

*Fluorescence Spectroscopy.* The fluorescence measurements were made using an SLM 8000c spectrofluorometer operated in the ratio mode. When making resonance energy transfer measurements between the IAF-$\beta\gamma_T$ and the EITC-$\alpha_T$GDP, the excitation wavelength was fixed at 460 nm and the emission spectrum was recorded from 480 to 610 nm. A typical energy transfer titration experiment was performed as follows: The IAF-$\beta\gamma_T$ was added (1–5 μL) to a buffer (200 μL) containing 20 mM HEPES, pH 7.4, and 5 mM $MgCl_2$ (assay buffer) to yield a final concentration of ~200 nM. Titrations were performed by adding successive aliquots (1–5 μL each) of the EITC-$\alpha_T$GDP species. The solutions were mixed and the emission spectra were recorded after each addition of the EITC-$\alpha_T$GDP. The peak fluorescence intensity was corrected for dilution; inner filter effects due to the addition of the EITC-$\alpha_T$GDP species were negligible (i.e., the absorbance at the excitation wavelength was always <0.02 absorbance unit). Energy transfer measurements that were used to monitor IAF-$\beta\gamma_T$ association with EITC-$\alpha_T$GDP, as an outcome of the dissociation of IAF-$\beta\gamma_T$ from an unlabeled $\alpha_T$GDP complex, were performed as outlined in the legends to Figures 3 and 5 in the Results section.

The tryptophan fluorescence of the $\alpha_T$GDP species was determined by exciting at 290 nm and reading the emission at 340 nm, as described in Phillips and Cerione (1988). The aluminum fluoride-induced changes were measured by adding small aliquots (1–10 μL) of a premixed solution of $AlCl_3$ (100 μM) and NaF (5 mM) to stirring $\alpha_T$GDP in assay buffer.

## RESULTS

The principal aim of these studies was to establish a fluorescence approach that would enable us to examine the kinetics of the dissociation of an activated $\alpha_T$ subunit from a $\beta\gamma_T$ subunit complex. In a previous study, we have used an $\alpha_T$GDP-induced enhancement in the fluorescence of a MIANS-labeled $\beta\gamma_T$ complex to monitor the interactions of the $\alpha_T$GDP species with the labeled $\beta\gamma_T$ (Phillips & Cerione, 1991). It was observed that, upon NaF addition, a rapid decrease in fluorescence was observed with a rate that was ~3-fold faster than that for intrinsic fluorescence changes in $\alpha_T$ under the same conditions [see Phillips and Cerione (1991), Figure 7]. However, because of the environmentally sensitive nature of the MIANS fluorescence, it was not possible to distinguish the dissociation of the $\alpha_T/\beta\gamma_T$ complex (that was induced by the activation of the $\alpha_T$ subunit) from conformational changes in the MIANS-$\beta\gamma_T$ species that might precede this dissociation event. In order to distinguish $\alpha_T/\beta\gamma_T$ association and dissociation events from conformational changes occurring within the G protein subunits, we have used environmentally insensitive fluorescent donor and acceptor chromophores in resonance energy transfer experiments.

*Use of EITC-Labeled $\alpha_T$GDP and IAF-Labeled $\beta\gamma_T$ as a Donor–Acceptor Pair for Resonance Energy Transfer.* The $\beta\gamma_T$ subunit complex contains reactive cysteine residues that can be labeled with different fluorescent cysteine reagents (Phillips & Cerione, 1991). The complete labeling of the $\beta\gamma_T$ cysteine residues has no effect on the ability of the $\beta\gamma_T$ complex to associate with the $\alpha_T$ subunit or to promote the rhodopsin-stimulated guanine nucleotide exchange activity of $\alpha_T$. The $\alpha_T$ subunit can be labeled at a reactive amino group (Hingorani & Ho, 1987), and recent peptide mapping studies indicate that the labeling occurs at lysine 267 (J. Erickson, unpublished observation). This modification of the $\alpha_T$ subunit has no apparent effect on its ability to bind to the effector enzyme although the labeled $\alpha_T$ subunit is no longer able to stimulate PDE activity (Erickson & Cerione, 1991). As will be demonstrated below, the labeled $\alpha_T$ subunit also retains its ability to bind to the $\beta\gamma_T$ complex.

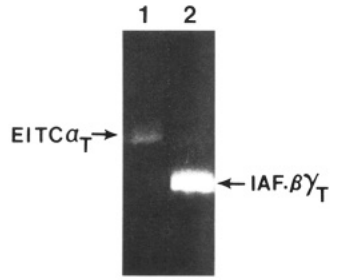


FIGURE 1: SDS–PAGE of the EITC-$\alpha_T$GDP and IAF-$\beta\gamma_T$ complex. The EITC-labeled $\alpha_T$GDP (2 $\mu$g) and the IAF-labeled $\beta\gamma_T$ (2 $\mu$g), prepared as described in the Materials and Methods section, were electrophoresed on an SDS–10% polyacrylamide gel and the fluorescent bands were photographed using a UV transilluminator.

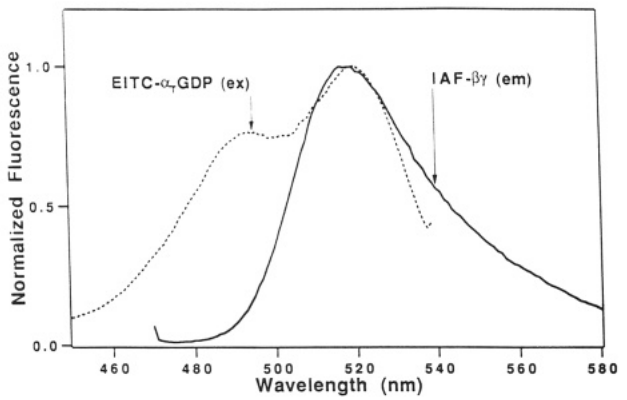


FIGURE 2: Normalized excitation and emission spectra of the EITC-$\alpha_T$GDP and the IAF-$\beta\gamma_T$. The emission spectrum for the IAF-$\beta\gamma_T$ (50 nM) was obtained by exciting the protein at 460 nm. The excitation spectrum was obtained by monitoring the emission at 518 nm. The excitation spectrum for the EITC-$\alpha_T$GDP species (50 nM) was obtained by recording the emission at 545 nm. The emission spectrum for the EITC-$\alpha_T$GDP complex was obtained by exciting the protein at 525 nm.

Resonance energy transfer approaches can serve as direct read-outs of protein–protein interactions, since the efficiency of energy transfer between a donor fluorophore and an acceptor chromophore is dependent on the distance separating the two. Our basic strategy for monitoring $\alpha_T/\beta\gamma_T$ interactions was to label the $\alpha_T$ subunit at its reactive lysine group and the $\beta\gamma_T$ complex at its reactive cysteine residues with appropriate donor and acceptor chromophores. In these studies, we have used an eosin isothiocyanate (EITC)-labeled $\alpha_T$GDP complex and an (iodoacetamido)fluorescein- (IAF-) labeled $\beta\gamma_T$. These subunit complexes were labeled and further purified by hydroxyapatite chromatography; Figure 1 shows an SDS–polyacrylamide gel of the fluorescent-labeled subunits. Figure 2 shows the spectral overlap of the fluorescence emission of the IAF-$\beta\gamma_T$ (i.e., the fluorescent donor) and absorption of the EITC-$\alpha_T$GDP (the energy transfer acceptor). As shown previously for the case of IAF-PDE and EITC-$\alpha_T$GTP$\gamma$S, the spectral overlap for protein conjugates of these two chromophores enables the direct measurement of the formation of protein complexes by resonance energy transfer (Erickson & Cerione, 1991).

The association of the EITC-labeled $\alpha_T$GDP with the IAF-labeled $\beta\gamma_T$ resulted in a quenching (typically 10–15%) of the IAF donor fluorescence, as an outcome of resonance energy transfer between the IAF and EITC labels (Figure 3A). The quenching of the IAF fluorescence by the EITC-$\alpha_T$GDP species was eliminated when the experiment was performed in the presence of a 5-fold excess of unlabeled $\beta\gamma_T$ (Figure 3B), presumably because the excess $\beta\gamma_T$ saturated the EITC-

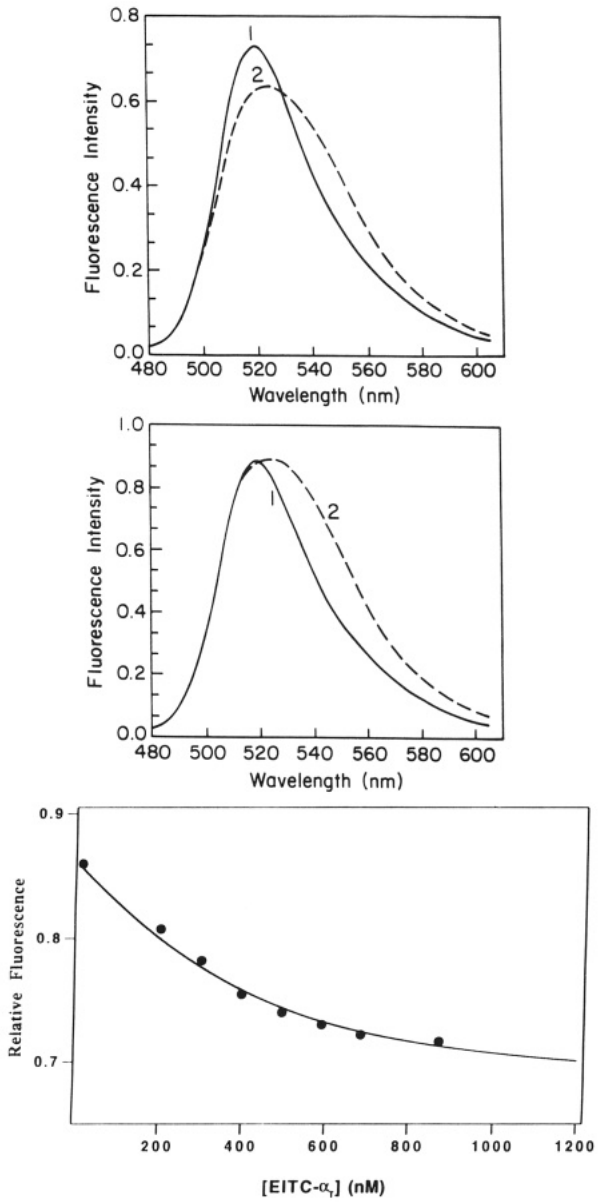


FIGURE 3: Quenching of the IAF-$\beta\gamma_T$ complex by the EITC-$\alpha_T$GDP. (A, top) Emission spectrum of the IAF-$\beta\gamma_T$ complex (200 nM) in the absence (spectrum 1) and presence (spectrum 2) of the EITC-$\alpha_T$GDP species (200 nM). (B, middle) Emission spectrum of the IAF-$\beta\gamma_T$ (200 nM) complex, alone (spectrum 1), and in the presence of 200 nM EITC-$\alpha_T$GDP and 900 nM (unlabeled) $\alpha_T$GDP (spectrum 2). (C, bottom) Titrations of the IAF-$\beta\gamma_T$ complex (200 nM) with the EITC-$\alpha_T$GDP species. The IAF-$\beta\gamma_T$ was titrated in 20 nM HEPES, pH 7.5, 5 mM $MgCl_2$, and 1 mM DTT with the indicated amounts of EITC-$\alpha_T$GDP. The data are plotted as the relative emission intensities of the IAF-$\beta\gamma_T$ at 518 nm (excitation 460 nm). The solid line shows the best fit to a simple bimolecular reaction [see eq 1 in Erickson and Cerione (1991)] and yields an apparent $K_d$ of 144 nM.

$\alpha_T$GDP and prevented it from binding to the donor-labeled $\beta\gamma_T$ complex. A significant reduction in the resonance energy transfer also occurred when the experiment was performed in the presence of excess, unlabeled $\alpha_T$GDP (see Figure 5B, below). The quenching of the IAF-$\beta\gamma_T$ fluorescence by the EITC-$\alpha_T$GDP species was saturable and the data could be fit to a simple model for a bimolecular reaction yielding an apparent $K_d$ value of $\sim$150 nM [147 nM $\pm$ 10 nM (Figure 3C)]. Previously, in studies using a MIANS-labeled $\beta\gamma_T$ complex, we reported that the association of $\alpha_T$GDP with $\beta\gamma_T$ was complete upon mixing the components (i.e., <2 s).

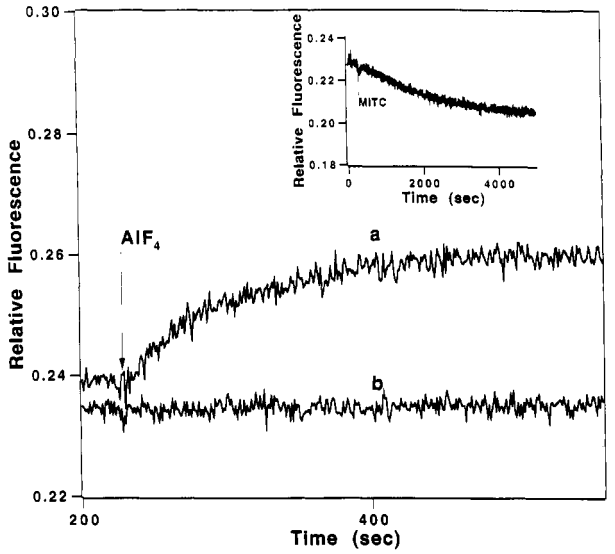


FIGURE 4: Modification of $\alpha_T$GDP at lysine 267 prevents aluminum fluoride-induced fluorescence enhancement. Samples of 250 nM $\alpha_T$GDP were equilibrated in stirred quartz cuvettes and excitation was fixed at 280 nm. Emission was monitored continuously at 340 nm and a 50-μL aliquot of premixed aluminum fluoride (final concentrations 3 μM $AlCl_3$ and 0.13 mM NaF) was added. The top curve (a) shows the tryptophan fluorescence of an unreacted sample of $\alpha_T$GDP while the aluminum fluoride response of the methyl isothiocyanate-reacted sample is shown in the lower trace (b). (Inset) Methyl isothiocyanate (2 μL) was added to a 10- × 10-mm quartz cuvette containing 2 mL of 20 mM HEPES, pH 7.4, and 5 mM $MgCl_2$ and 20 μL of a 25 μM stock (~250 nM final concentration) of $\alpha_T$GDP. The reaction was allowed to proceed for 2 h while the 340-nm emission of the sample was monitored.

Moreover, the titration data indicated a binding constant for unlabeled $\alpha_T$GDP and MIANS-$\beta\gamma_T$ of ~300 nM, in approximate agreement with the affinity of these two proteins reported in the present study. The same rapid rate of binding was also observed when monitoring the association of the EITC-$\alpha_T$GDP species with IAF-$\beta\gamma_T$ through resonance energy transfer (data not shown).

*Kinetics of the Dissociation of an Activated $\alpha_T$ Subunit from $\beta\gamma_T$.* The modification of lysine 267 of $\alpha_T$ (i.e., to form the EITC-$\alpha_T$GDP species) prevents the activation of the $\alpha_T$ subunit either by rhodopsin (plus GTP) or by aluminum fluoride. This is illustrated by the data in Figure 4 where the intrinsic fluorescence of the $\alpha_T$ subunit was monitored with or without prior reaction with the smaller, nonfluorescent methyl analog of isothiocyanate. The lower curve in Figure 4 demonstrates that the modification of lysine 267 eliminates the increase in the fluorescence of $\alpha_T$ tryptophan 207 that reflects an activating conformational change in the $\alpha_T$ subunit and is normally induced upon the addition of aluminum fluoride to purified $\alpha_T$ (Faurobert et al., 1993). The time course for $\alpha_T$ modification with the nonfluorescent methyl isothiocyanate (MITC) analog is shown in the inset to Figure 4. The reaction time course observed for either eosin or fluorescein isothiocyanate, where the reaction was complete after 1.5–2 h [25 °C, pH = 8.0; see Materials and Methods and Hingorani and Ho (1987)], was similar to the decreasing curve of 340-nm emission shown here.

The fact that only the unmodified form of $\alpha_T$ can be activated (and thereby induced to dissociate from the holotransducin complex) following aluminum fluoride addition offers a way to probe the kinetics of transducin subunit exchange. Specifically, we have compared the rate for G protein subunit dissociation with the rate for the activation of the $\alpha_T$ subunit, using the experimental approach depicted schematically in Figure 5A. The first step entails the association of an unlabeled $\alpha_T$GDP subunit with an IAF-labeled $\beta\gamma_T$ complex, which occurs on the time scale of mixing in these experiments as noted above. The holo-$\alpha_T$GDP/IAF-$\beta\gamma_T$ species can then be activated by the addition of 100 μM $AlCl_3$ and 10 mM NaF. Using aluminum fluoride to activate $\alpha_T$ has the advantage of enabling the total $\alpha_T$GDP subunit pool to be activated simultaneously rather than catalytically (i.e., through rhodopsin-facilitated exchange). Furthermore, the rate of the aluminum fluoride-induced activation event is not immediate (i.e., within the time period of mixing) but rather occurs on a time scale of several seconds, providing an easily measured time course and an accurate comparison of the rates of activation (as defined by intrinsic fluorescence changes in $\alpha_T$) and subunit dissociation (measured with the aid of energy transfer between EITC-$\alpha_T$ and IAF-$\beta\gamma_T$). The proposed subunit dissociation event that accompanies aluminum fluoride binding should generate an $\alpha_T$GDP/aluminum fluoride species and a free IAF-$\beta\gamma_T$ complex. In the reaction sequence shown, the free IAF-$\beta\gamma_T$ so generated is then able to reassociate with an EITC-$\alpha_T$GDP species which remains in the inactive conformation due to its inability to be activated by aluminum fluoride (Figure 4).

Figure 5B shows three emission spectra of IAF-$\beta\gamma_T$ under these experimental conditions. Spectrum 1 shows the original IAF-$\beta\gamma_T$ fluorescence and spectrum 2 shows the IAF fluorescence in the presence of EITC-$\alpha_T$GDP and excess, unlabeled $\alpha_T$GDP. Under these conditions, there is little or no quenching of the IAF-$\beta\gamma_T$ fluorescence (<3%) by the EITC-$\alpha_T$GDP species, demonstrating the competitive binding of the modified and native $\alpha_T$ species for IAF-$\beta\gamma_T$. However, upon the addition of aluminum fluoride, the resonance energy transfer quenching normally observed between the IAF-$\beta\gamma_T$ and EITC-$\alpha_T$GDP is restored (spectrum 3). In control experiments, no quenching of the IAF fluorescence is observed when aluminum fluoride is added to the IAF-$\beta\gamma_T$ complex, alone (data not shown). Thus, the rapid (aluminum fluoride-stimulated) quenching that occurs when free EITC-$\alpha_T$GDP binds to the newly dissociated IAF-$\beta\gamma_T$ provides a way to assess the kinetics of the rate-limiting step in this reaction sequence, namely, the dissociation of aluminum fluoride-activated holotransducin.

Figure 6A shows the time course for the aluminum fluoride-induced fluorescence changes in the $\alpha_T$GDP/IAF-$\beta\gamma_T$ complex, as reflected by the enhancement of the $\alpha_T$ tryptophan fluorescence that accompanies the activation event (Phillips & Cerione, 1988). As illustrated by the solid curve in Figure 6A, the data can be well-described by a single exponential, yielding a rate constant of 0.03 $s^{-1}$ ($t_{1/2}$ = 23.3 s). This indicates that the aluminum fluoride-induced conformational change that accompanies activation requires >23 s for completion, consistent with other published time courses using enhanced fluorescence as a readout for $\alpha_T$ activation [cf. Higashijima et al. (1987)]. Figure 6B shows the time course for the association of the IAF-$\beta\gamma_T$ complex (generated as an outcome of its dissociation from aluminum fluoride-activated $\alpha_T$ subunit) with the EITC-$\alpha_T$GDP, as reflected by the energy transfer quenching of the IAF fluorescence. This time course also is well-fitted by a signal exponential, although this response to activating concentrations of $AlCl_3$ and NaF occurs approximately 1 order of magnitude faster, with a rate constant of 0.25 $s^{-1}$ ($t_{1/2}$ = 2.8 s). Taken together, these results suggest that there are two distinct conformational transitions following the initial binding of aluminum fluoride complexes by $\alpha_T$ and indicate that G protein subunit dissociation occurs prior to

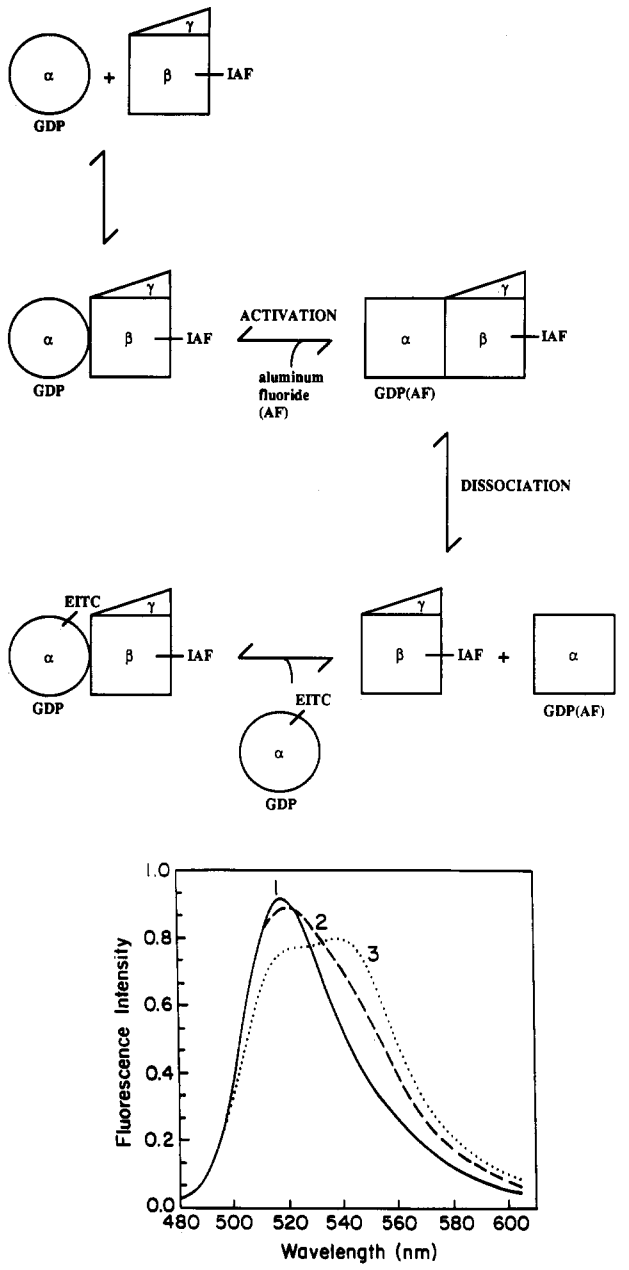


FIGURE 5: Aluminum fluoride-induced activation of $\alpha_T$GDP and the subsequent dissociation of the activated $\alpha_T$GDP-aluminum fluoride species from the IAF-labeled $\beta\gamma_T$ complex. (A, top) Schematic depicting the steps underlying the aluminum fluoride-induced dissociation of an IAF-$\beta\gamma_T$ complex from an activated $\alpha_T$ subunit. The first step involves the formation of a holotransducin complex from the $\alpha_T$GDP and IAF-labeled $\beta\gamma_T$ complex. Previous studies have shown that the IAF-labeled $\beta\gamma_T$ is able to effectively couple to $\alpha_T$ subunits. The next step involves the aluminum fluoride-induced activation of $\alpha_T$, which stimulates the dissociation of the labeled $\beta\gamma_T$ from the $\alpha_T$GDP/aluminum fluoride complex. This step can be performed in the presence of EITC-$\alpha_T$GDP, since the labeled $\alpha_T$ subunit does not respond to aluminum fluoride. The generation of the IAF-$\beta\gamma_T$, due to the G protein subunit dissociation event, can then be measured by the energy transfer that occurs between the IAF and EITC moieities, upon the immediate formation of the EITC-$\alpha_T$GDP/IAF-$\beta\gamma_T$ complex. (B, bottom) Demonstration that the addition of aluminum fluoride induces the dissociation of an IAF-$\beta\gamma_T$ complex from an activated $\alpha_T$ subunit using resonance energy transfer. Spectrum 1 shows the fluorescence emission of the IAF-$\beta\gamma_T$ complex (200 nM) alone. Spectrum 2 shows the emission of the IAF-$\beta\gamma_T$ complex in the presence of 900 nM (unlabeled) $\alpha_T$GDP and 200 nM EITC-$\alpha_T$GDP, prior to the addition of 100 $\mu$M $AlCl_3$ and 5 mM NaF (to generate the aluminum fluoride complex), and spectrum 3 shows the emission of the IAF-$\beta\gamma_T$ (recorded for 5 min) after the addition of $AlCl_3$ and NaF.

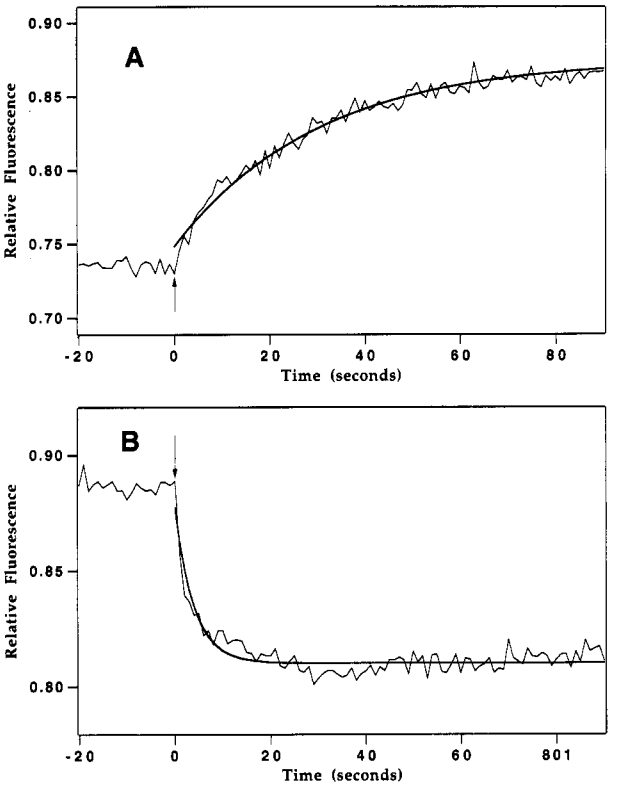


FIGURE 6: Kinetics of aluminum fluoride-induced transducin activation and subunit dissociation. (A) Time course of the aluminum fluoride-induced fluorescence enhancement of the $\alpha_T$GDP complex. The tryptophan fluorescence of the purified $\alpha_T$GDP complex (~900 nM) in 20 mM HEPES, pH 7.5, 5 mM $MgCl_2$, and 1 mM DTT was obtained by exciting at 280 nm and then monitoring the emission at 340 nM. At the time indicated by the arrow, $AlCl_3$ (100 $\mu$M) and NaF (5 mM) were added to yield the $\alpha_T$GDP-aluminum fluoride species. The solid line represents the best fit obtained using the equation $F(t) = F_0 + F_1(1 - \exp^{-k_{act}t})$, where $F(t)$ is the tryptophan fluorescence emission of $\alpha_T$GDP at time $t$, $F_0$ is the initial level of $\alpha_T$GDP fluorescence before aluminum fluoride addition, $F_1$ is the total observed change in emission, and $k_{act}$ is the rate constant for the activation of $\alpha_T$ as monitored by the change in tryptophan fluorescence. The parameters obtained from the fitting procedure are $F_0 = 0.75$, $F_1 = 0.13$, and $k_{act} = 0.03$. (B) Resonance energy transfer measuring the association of an EITC-$\alpha_T$GDP species with an IAF-$\beta\gamma_T$ complex, generated by an aluminum fluoride-stimulated G protein subunit dissociation event. This experiment was performed as described in Figure 5A. [$\alpha_T$GDP] = 900 nM; [IAF-$\beta\gamma_T$] = 200 nM; and [EITC-$\alpha_T$GDP] = 200 nM. The time course for resonance energy transfer between the EITC-$\alpha_T$GDP and IAF-$\beta\gamma_T$ (excitation = 460 nm, emission = 518 nm) was initiated by the addition of 100 $\mu$M $AlCl_3$ and 5 mM NaF. The measurements were performed in 20 mM HEPES, pH 7.5, 5 mM $MgCl_2$, and 1 mM DTT. The solid line shows the best fit of the data to a single rate constant describing this dissociation according to the equation $F(t) = F_0 + F_1(\exp^{-k_{act}t})$, where the parameters are defined in panel A, except that $F_0$ is now the final level of fluorescence following the exchange of subunits. The parameters for the curve shown are $F_0 = 0.81$, $F_1 = 0.07$, and $k_{act} = 0.25$.

the aluminum fluoride-induced changes in the intrinsic fluorescence of the $\alpha_T$ subunit.

## DISCUSSION

It has been well established that heterotrimeric G proteins shuttle between cell surface receptors and effector proteins to mediate receptor regulation of biological responses. The G protein $\alpha$ subunits are known to stimulate a number of effectors including adenylyl cyclase, the cyclic GMP phosphodiesterase, phospholipase C-$_{\beta 1}$, and ion channels (Stryer, 1991; Khorana, 1992; Lefkowitz & Caron, 1988; Gilman, 1987; Smrcka et

al., 1991; Taylor et al., 1990; Brown & Birnbaumer, 1990). Likewise, it has been suggested that the G protein βγ complexes can regulate effector activities, the best known examples being the inhibition of adenylyl cyclase through the βγ deactivation model (Gilman, 1987) and the stimulation of specific isoforms of adenylyl cyclase (Tang & Gilman, 1991; Gao & Gilman, 1991). The ability of the different subunit components of heterotrimeric G proteins to act as regulators of effector activity raises the important issue of the rate of G protein subunit dissociation and how it compares to the rate of G protein activation and effector binding.

In order to address this issue, we have set out to use fluorescence approaches to compare the relative rates for the activation of a holo-G protein complex and the ensuing dissociation of the activated α subunit from the $\beta\gamma_T$ complex. We have used the vertebrate phototransduction pathway as a model for these studies and first examined $\beta\gamma_T$ subunit complexes that were labeled with environmentally sensitive reporter groups (Phillips & Cerione, 1991). The $\beta\gamma_T$ complex initially was chosen because we (Phillips & Cerione, 1992; Phillips & Cerione, 1991) and others (Ho & Fung, 1984) had found that the cysteine residues of this complex could be modified without any detectable effects on $\beta\gamma_T$ function. We found that an $\alpha_T$GDP-induced enhancement of the MIANS-$\beta\gamma_T$ fluorescence could be used to read out the formation of the holotransducin complex from its subunit components (Phillips & Cerione, 1991). The activation of the $\alpha_T$ subunit either by aluminum fluoride or by rhodopsin plus GTP (or GTPγS) resulted in a reversal of the $\alpha_T$GDP-induced enhancement of the MIANS fluorescence, presumably reflecting the dissociation of the activated $\alpha_T$ subunit from the MIANS-$\beta\gamma_T$. In the case of aluminum fluoride-induced activation, the change in MIANS fluorescence was rapid, reaching completion in <10 s under conditions similar to those used in the present study. However, it was difficult to use the changes in MIANS-$\beta\gamma_T$ fluorescence to draw conclusions regarding the kinetics of G protein subunit association and dissociation events, since these fluorescence changes may reflect conformational changes in the local environment of the MIANS probes that occur with rates distinct from those for the binding or dissociation of the G protein subunits.

This then prompted us to develop an approach that uses changes in resonance energy transfer between fluorescently labeled $\alpha_T$ and $\beta\gamma_T$ complexes to directly monitor G protein subunit association–dissociation events. The efficiency of energy transfer is dependent on the proximity of the donor fluorophore and an acceptor chromophore (Cantley & Hammes, 1975), and in previous studies we have taken advantage of this to read out the interactions between a donor-labeled PDE molecule and an acceptor-labeled $\alpha_T$GTPγS species (Erickson & Cerione, 1991). In the case of $\alpha_T/\beta\gamma_T$ interactions, the strategy was to label the cysteine residues of the $\beta\gamma_T$ complex with a fluorescent donor moiety (i.e., IAF) and the reactive lysine residue of the $\alpha_T$ subunit with an appropriate acceptor, EITC. As shown in Figure 4, the EITC-$\alpha_T$ subunit cannot be directly activated. However, the exchange of an EITC-labeled $\alpha_T$ subunit, for an unlabeled $\alpha_T$ subunit within an $\alpha_T$/IAF-$\beta\gamma_T$ complex, which occurs as an outcome of the dissociation of the activated $\alpha_T$/IAF-$\beta\gamma_T$ complex, can be monitored as outlined in Figure 5A. The use of aluminum fluoride to activate $\alpha_T$ subunits of heterotrimeric G proteins has been well established (Phillips & Cerione, 1988; Higashijima et al., 1987). In the case of transducin, the aluminum fluoride-induced activation event, either as reflected by an enhancement of the tryptophan fluorescence of $\alpha_T$ or by a stimulation of PDE activity, requires several seconds.

Our experiments indicate that there are effects of aluminum fluoride complex binding to $\alpha_T$GDP that precede the change in tryptophan 207 fluorescence. Specifically, we find that the aluminum fluoride-bound $\alpha_T$ subunit dissociates from the IAF-$\beta\gamma_T$ complex with a rate that is significantly faster than that for the aluminum fluoride-induced enhancement of the $\alpha_T$ tryptophan fluorescence. This indicates that different regions of the $\alpha_T$ subunit do not simultaneously sense the occupation of this activating ligand. Available biochemical evidence suggests that G protein βγ complexes bind to the amino-terminal domains of α subunits, whereas the effectors appear to bind within the carboxyl terminal domains (Gilman, 1987). Both βγ and effector interactions are tightly regulated by ligands that activate G protein α subunits and consequently both the amino- and carboxyl-terminal domains of α subunits must be influenced by activating conformational changes.

The recent X-ray crystallographic studies by Noel et al. (1993) suggest that the binding of activating ligands to the $\alpha_T$ subunit (i.e., at the binding site for the γ-phosphate of GTP) triggers conformational changes that are felt at the α2 helix, as reflected by an enhancement of the fluorescence of tryptophan 207, and that this change is propagated through the α3 and α4 helices to a region within the carboxyl-terminal domain of $\alpha_T$ (amino acid residues 293–314) that is essential for binding to and stimulating the PDE (Rarick et al., 1992). If, as has been suggested, it is the $AlF_3OH^-$ species that complexes with the bound GDP of $\alpha_T$ (Antonny & Chabre, 1992), our results would suggest that this interaction occurs rapidly and immediately directs changes in the amino-terminal domain of $\alpha_T$ that trigger the release of $\beta\gamma_T$. The slower condensation of the $AlF_3OH^-$ species with the β-phosphate of GDP, whereby the $AlF_3OH^-$ complex now assumes an unfavored tetrahedral geometry (Antonny & Chabre, 1992), may then represent the molecular event that induces the changes in the α2–α4 helices that lead to the enhanced fluorescence and the activation of the effector enzyme (i.e., the cGMP PDE). It would be expected that GTP could induce the latter conformational change more rapidly than aluminum fluoride because it does not need to undergo a condensation reaction. Studies using reconstituted phospholipid vesicle systems containing purified rhodopsin in fact suggest that at relatively high levels of rhodopsin ([rhodopsin] ~ $[\alpha_T]$) the GTP-dependent enhancement of the tryptophan fluorescence is rapid (Guy et al., 1990). However, it is difficult to obtain definitive results because, at high levels of rhodopsin, the background rhodopsin tryptophan fluorescence interferes with the $\alpha_T$ tryptophan signal, and lower levels of rhodopsin ([rhodopsin] ≪ $[\alpha_T]$) limit the rate of $\alpha_T$ subunit activation (Guy et al., 1990). It is interesting that the rate of the aluminum fluoride-induced enhancement of the $\alpha_T$ tryptophan fluorescence is similar to the rate determined for the GTP hydrolytic event. While the similarity in these rates raises the possibility that the change in the $\alpha_T$ tryptophan fluorescence reflects a conformational change that is rate-limiting for GTP hydrolysis, this possibility seems unlikely given that the studies using reconstituted rhodopsin suggest that the GTP-induced enhancement of the $\alpha_T$ tryptophan fluorescence is not rate-limiting for the GTPase reaction (Guy et al., 1990). We suggest, however, that the aluminum fluoride-induced conformational changes in G protein α subunits may represent the sequence of molecular events that occur in a more physiological setting. The sequential changes in the conformational of the $\alpha_T$ subunit, following GTP binding, would

likewise result in $\beta\gamma$ dissociation prior to a second conformational change that primed the free $\alpha$GTP species for binding to its biological effector. We suspect that the first of these conformational changes (resulting in the dissociation of $\beta\gamma_T$) may not be prerequisite for the second (tryptophan enhancement), since previous studies by Frey et al. (1988) using Cr(III)GTP have suggested that transducin activation can occur in the absence of subunit dissociation.

In summary, the results reported here suggest that G protein subunit dissociation is an early outcome of G protein activation via aluminum fluoride and occurs before the $\alpha_T$ has undergone the necessary change in its tertiary structure to exhibit the enhanced tryptophan fluorescence characteristic of the activated state. This is consistent with the proposal (Gilman, 1987) that it is the G protein $\alpha_T$ subunit, rather than the holotransducin complex, which contacts the effector PDE. In the future, our efforts will be directed toward comparing the rates of the G protein subunit dissociation event, and the dissociation of the activated $\alpha_T$ subunit from rhodopsin, with the rate for $\alpha_T$/effector interactions. Such studies, coupled with what promises to be rapid progress in understanding the structural basis of observed $\alpha$-transducin function, will further our understanding of the mechanisms underlying G-protein-mediated signal transduction.

## ACKNOWLEDGMENT

We would like to thank Ms. Deidre Heyser for technical support and Ms. Cindy Westmiller for secretarial assistance.

## REFERENCES

Antonny, B., & Chabre, M. (1992) *J. Biol. Chem. 267*, 6710–6718.

Arshavsky, V. Y., & Bownds, M. D. (1992) *Nature 357*, 416–417.

Brown, A. M., & Birnbaumer, L. (1990) *Annu. Rev. Physiol. 52*, 97.

Cantley, L. C., & Hammes, G. (1975) *Biochemistry 14*, 2976–2981.

Erickson, J. W., & Cerione, R. A. (1991) *Biochemistry 30*, 7112–7118.

Faurobert, E., Otto-Bruc, A., Chardin, P., & Chabre, M. (1993) *EMBO J. 12*, 4191–4198.

Frey, S. E., Hingorani, V. N., Su-Tsai, S.-M., & Ho, Y.-K. (1988) *Biochemistry 27*, 8209–8218.

Gao, B., & Gilman, A. G. (1991) *Proc. Natl. Acad. Sci. U.S.A. 88*, 10178–10182.

Gierschik, P., Simons, C., Woodward, C., Somers, R., & Spiegel, A. (1984) *FEBS Lett. 172*, 321–325.

Gilman, A. G. (1987) *Annu. Rev. Biochem. 56*, 615–649.

Guy, P. M., Koland, J., & Cerione, R. (1990) *Biochemistry 29*, 6954–6964.

Higashijima, T., Ferguson, K. M., Sternweis, P. C., Ross, E. M., Smigel, M. D., & Gilman, A. G. (1987) *J. Biol. Chem. 262*, 752–756.

Hingorani, V., & Ho, Y. (1987) *Biochemistry 26*, 1633–1639.

Ho, Y.-K., & Fung, B. K. K. (1984) *J. Biol. Chem. 259*, 6694–6699.

Khorana, H. G. (1992) *J. Biol. Chem. 267*, 1–4.

Kroll, S., Phillips, W. J., & Cerione, R. (1989) *J. Biol. Chem. 264*, 4490–4497.

Lefkowitz, R. J., & Caron, M. G. (1988) *J. Biol. Chem. 263*, 4993–4996.

Noel, J. P., Hamm, H. E., & Sigler, P. B. (1993) *Nature 366*, 654–663.

Phillips, W. J., & Cerione, R. A. (1988) *J. Biol. Chem. 263*, 15498–15505.

Phillips, W. J., & Cerione, R. A. (1991) *J. Biol. Chem. 266*, 11017–11024.

Phillips, W. J., & Cerione, R. A. (1992) *J. Biol. Chem. 267*, 17032–17039.

Phillips, W. J., Trukawinski, S., & Cerione, R. A. (1989) *J. Biol. Chem. 264*, 16679–16688.

Pines, M., Gierschik, P., Milligan, G., Klee, W., & Spiegel, A. M. (1985) *Proc. Natl. Acad. Sci. U.S.A. 82*, 4095–4099.

Rarick, H. M., Artemyev, N. O., & Hamm, H. E. (1992) *Science 256*, 1031–1033.

Smrcka, A. V., Hepler, J. R., Brown, K. O., & Sternweis, P. D. (1991) *Science 251*, 804–807.

Stryer, L. (1991) *J. Biol. Chem. 266*, 10711–10714.

Tang, W.-J., & Gilman, A. G. (1991) *Science 254*, 1500–1503.

Taylor, S. J., Smith, J. A., & Exton, J. H. (1990) *J. Biol. Chem. 265*, 17150–17156.